National Defence / Défense nationale

INVESTIGATION OF ALPHA PARTICLE INDUCED SINGLE-EVENT UPSETS IN CHARGE-COUPLED DEVICES (U)

by

G.T. Pepper and A. Fechete
Nuclear Effects Section
Electronics Division

DEFENCE RESEARCH ESTABLISHMENT OTTAWA
REPORT NO. 1114

PCN
041LS

December 1991
Ottawa

92-02510/

ABSTRACT

The mechanisms for generation of single-event upsets (SEUs) in a linear charge-coupled device (CCD) were studied through irradiation with monoenergetic 5.48 MeV alpha particles from a very low flux ^{241}Am source. Spatial correlation ("cluster" analysis) of soft errors due to single alpha particle hits was demonstrated to be a necessary prerequisite for quantitative analysis of different SEU error-generating phenomena. The Texas Instruments TC-103 virtual phase CCD used in this study is shown to be sensitive to alpha particles not only in the vicinity of photo-sites as expected, but also in the transport CCDs This latter effect may have adverse consequences for applications employing CCDs as position-sensitive ionizing radiation detectors. The techniques developed in this work for the analysis of one dimensional arrays is readily extensible to two dimensional CCD arrays.

RÉSUMÉ

Nous avons étudié les méchanismes de la génération des renversements d'évènement unique (SEU) dans un système de transfert de charge linéaire(CCD) en se servant d'une source de radiation Am-241 aux particules monoénergétiques de 5.48 MeV.

Nous avons démontré que la corrélation spatiale des erreurs (molles) due à des collisions de particules alpha simple etait une condition préalable nécessaire à l'analyse quantitative du pourcentage d'erreur du SEU. L'appareil Texas Instruments TC-103, CCD à phase virtuelle, utilisé dans cet étude démontre qu'il est sensible aux particles alpha, non seulement près des photo-sites mais aussi dans les voies de transport. Ce dernier effet peut avoir des conséquences négatives si nous employons ces CCD comme des détecteurs de radiation ionisante. Les techniques que nous avons développées et employées pour l'étude des CCD à matrice un-uni-dimentionnelle sont également employées pour les CCD à matrice bi-dimensionnelle.

EXECUTIVE SUMMARY

Charge-coupled devices (CCDs) find wide application in military and commercial imaging and sensor applications. These devices are used extensively in satellite-based remote sensing systems. Generation of errors in these devices can occur by the interaction of ionizing radiation with the semiconductor material of the CCD. Since the output of these sensors is usually of consequence, understanding how ionizing radiation produces errors in CCDs is of great importance, especially since the data artifacts are indistinguishable from "real" data.

This report summarizes the experimental and analytical techniques used to investigate the creation of errors in a linear array CCD by one form of ionizing radiation - energetic alpha particles. These particles are not unlike the particulate ionizing radiation that space vehicles are subjected to in the near-earth environment. A significant new error generation mechanism was discovered, in the particular CCD used in this study, that may limit the usefulness of this CCD in some critical sensor applications.

TABLE OF CONTENTS

	PAGE
ABSTRACT/RÉSUMÉ	iii
EXECUTIVE SUMMARY	v
TABLE OF CONTENTS	vii
LIST OF FIGURES	ix
LIST OF TABLES	xv
1.0 INTRODUCTION	1
2.0 DESCRIPTION AND OPERATION OF THE TC-103 VIRTUAL PHASE LINEAR CCD	3
3.0 EXPERIMENTAL SYSTEM	6
4.0 EXPERIMENTAL RESULTS	9
4.1 ALPHA PARTICLE IRRADIATION OF THE ENTIRE CCD ARRAY	9
4.2 SINGLE SLIT EXPERIMENT	16
5.0 CONCLUSION	18
FIGURES	20
REFERENCES	37

LIST OF FIGURES

PAGE

Figure 1. Functional block diagram of the Texas Instruments TC-103 2048 element, virtual phase charge-coupled device. 20

Figure 2. Operating input and output waveforms for the Texas Instruments TC-103 CCD. 21

Figure 3. A vertical cross-section of the TC-103 CCD in the vicinity of two adjacent pixels. The clocked and virtual well/barrier regions are indicated for one pixel. 22

Figure 4. Illustration of the mechanism used to linearly transfer charge in the TC-103 virtual phase CCD. The voltage potential profile (ϕ) in the virtual barrier/well regions is not influenced by the gate potential. 23

Figure 5. Block diagram of the experimental system employed in this work to investigate alpha particle induced SEUs in the TC-103 CCD. . . 24

Figure 6. Typical output waveforms from the TC-103 CCD, captured by a 300 MHz digital oscilloscope, for a single alpha particle induced a) single pixel hit, b) hit on an adjacent pair of pixels and c) transport CCD pixel hit. The different types of pixel hits are explained in the text. 25

Figure 7. A typical "raw" pulse-height spectrum obtained for alpha particle induced SEUs in the TC-103 CCD. No data processing (e.g. spatial correlation or "cluster analysis") was performed on the raw data. The integral number of events recorded in the spectrum was 138,022. 26

Figure 8. A pulse-height spectrum of isolated single pixel hits. This is for the same experimental run as presented in Figure 7. The integral number of events recorded in the spectrum was 67,675. 27

Figure 9. The same experimental data as in Figure 8, but the pulse-height spectrum of single pixel hits have been corrected for d.c. offset and charge transfer inefficiency (CTI), resulting in improved resolution of the peak. The pulse-height for even and odd pixels is also shown. The integral number of counts recorded in the spectrum was 67,675 (33,876 even pixel hits+33,779 odd pixel hits). 28

Figure 10. Spatial distribution of single pixel alpha particle hits for the data presented in Figure 9. The distribution is peaked towards the middle of the array due to differences in source-pixel solid angles. The "point" source was located directly above the linear array, near the centre. 29

Figure 11. A pulse-height distribution for alpha particle induced adjacent pixel hits. The pulse-height shown represents the summed pulse-height of each even/odd pixel pair that forms an adjacent pixel hit. The data is for the same experimental run as in previous Figures and has been corrected for d.c. offset and CTI. Even and odd pixel pulse-height distributions are also shown. The integral number of events recorded in the spectrum is 12,884 (6,308 even pixels had the larger pulse-height of the even/odd pixel pairs and 6,576 odd pixel had the larger pulse-height of the even/odd pixel pairs). 30

Figure 12. A pulse-height distribution for alpha particle induced transport CCD pixel hits. The pulse-height shown represents the summed pulse-height of each 2 pixels (i.e. pixel 'n' and pixel 'n+2') that form a transport CCD pixel hit. The data is for the same experimental run as in previous Figures and has been corrected for d.c. offset and CTI. Even and odd pixel pulse-height distributions are also shown. The integral number of events recorded in the spectrum is 20,837 (6,308 even pixels had the larger pulse-height of the even/odd pixel pairs and 6,576 odd pixel had the larger pulse-height of the even/odd pixel pairs). 31

Figure 13. Spatial distribution of transport CCD pixel hits for the same data presented in Figure 12. 32

Figure 14. A pulse-height spectrum of alpha particle induced single pixel hits for the TC-103 CCD that has been covered, except for a narrow slit opening in the middle of the array. The 5.48 MeV alpha particles have insufficient energy to penetrate the thickness of the metal shield used. The data has been corrected for d.c. offset and charge transfer inefficiency (CTI). The pulse-height for even and odd pixels is also shown. . . . 33

Figure 15. Spatial distribution of alpha particle induced single pixel hits for the narrow single slit experiment. The data is from the same experimental run as for the data presented in Figure 14. 34

Figure 16. Spatial distribution of alpha particle induced adjacent pixel hits for the narrow single slit experiment. The data is from the same experimental run as for the data presented in Figure 14. 35

Figure 17. Spatial distribution of alpha particle induced transport CCD pixel hits for the narrow single slit experiment. The data is from the same experimental run as for the data presented in Figure 14. 36

LIST OF TABLES

PAGE

Table 1. Classification of the type of pixel hit by output pixel sequences from CCD. These event sequences are caused by a single alpha particle interaction in the CCD. 11

Table 2. Relative occurrence of single, adjacent, transport CCD and "other" types of pixel hits for data presented in Figures 9 through 13. 14

1.0 INTRODUCTION

Charge-coupled devices (CCDs), based on metal oxide semiconductor (MOS) technology, have found wide application in modern commercial and military imaging and signal processing systems since their introduction by Bell Laboratories in 1970 [1]. Charge-coupled devices continue to dominate an ever-increasing variety of scientific and engineering applications, ranging from detection of ionizing radiation to visible light spectroscopy [2]. Over the past two decades, much effort has been expended characterizing the performance of CCDs as a function of total dose [3-9] in ionizing radiation environments, especially for space-based applications. Recently, research has been focused on the response of CCDs to soft [10-13] and hard [14-16] x-rays, as well as very high energy charged particles [17-19] for use as position-sensitive detectors. To date, however, minimal effort has been directed towards the investigation of ion-induced single-event upsets (SEUs) in CCDs [20-22], the subject of concern of this report.

Analogous to ion-induced soft errors in memory devices, CCDs are vulnerable to the passage of charged particles. For both the CCD and the memory device, the soft error rate is dependent upon factors such as the cell's dimensions, the stopping power (dE/dx) or linear energy transfer (LET) of the incident ion and the charge collection efficiency. Unlike a memory device which has a critical charge (Q_c) that determines the logic state and soft-error threshold, the analog output of the CCD can span a large dynamic range, typically 1,000:1 or greater [2]. Between the noise floor and saturation level of the CCD, the analog output signal varies linearly with the charge collected in the sensitive volume [23]. Thus, the CCD provides a unique opportunity for continuous analog domain observation of charged particle interactions in MOS devices.

The use of CCDs for detector applications in ionizing radiation environments poses unique problems. Applications using one and two-dimensional CCD arrays for imaging and position-sensitive ionizing radiation detection rely upon the integrity of the spatial data from the CCD. Thus, it is important to characterize and quantify the CCD output in terms of false events and/or corrupted data when the CCD is subjected to an undesirable ionizing radiation background. Such circumstances are typically encountered by CCDs used in space-borne systems, where adequate device shielding cannot be provided. In ionizing radiation detection systems employing CCDs, the radiation which is detected is also capable of inducing spurious data artifacts in the CCD via other physical mechanisms.

In this report, single, monoenergetic alpha particle induced SEU effects on the Texas Instruments (TI) TC-103 2048 pixel, linear CCD are described. Unlike previous work conducted in this field [20-22], spatial correlation or cluster analysis was conducted to yield pulse-height distributions, enabling evaluation of device performance that would otherwise be difficult or impossible to accomplish. Spatial correlation techniques are also shown to considerably improve the energy resolution of the CCD beyond that obtained by simple pulse-height analysis, for charged particle spectroscopic applications.

The TC-103 CCD was selected for this study for several reasons. The TC-103 is a representative device from a family of one and two-dimensional CCD arrays, based on buried n-channel, virtual phase (VP) technology [24, 25]. The VP technology has been demonstrated to be relatively radiation hard [3], compared to typical CCD technologies. Because of the rad-hardness, simplified operation and reliability of the VP technology, TI devices have been

selected for use in several space missions. The TI TC-104 linear array (similar to the TC-103, but with 3456 pixels) has been flown in the MEOSS (Monocular Optoelectronic Multispectral Scanner) camera [23]. A TI 800x800 pixel VP CCD was flown in the planetary imager for the 1985 Galileo spacecraft mission [26]. Non-TI versions of buried n-channel, linear CCDs have been flown on numerous other missions including the GIOTTO HMC [27] (Halley Multicolor Camera) and the SPOT [28] satellite.

2.0 DESCRIPTION AND OPERATION OF THE TC-103 VIRTUAL PHASE LINEAR CCD

A functional block diagram of the Texas Instrument TC-103 linear CCD is shown in Figure 1. The TC-103 incorporates virtual-phase MOS technology [24, 25], which requires less complex drive electronics than other traditionally designed CCDs, because of its simplified clocking requirements. This feature will be described in more detail following a general summary of the device's features and operation.

The linear array of sensor elements (pixels or photo-sites) consists of 2048 photosensitive areas. Each pixel measures 12.7 microns square, with approximately 12.7 microns between centres. Electron-hole pairs are generated by interaction of incident ions (or any other radiation with sufficient energy to create an electron-hole pair) in the single-crystal silicon. The electrons are subsequently collected in the sensor element(s) and the holes are swept into the substrate. The amount of charge accumulated in each pixel is a function of the incident ion flux, ion energy and exposure time.

The transfer gates, which are adjacent to the linear

array of photo-sites, are used to transfer the charge packets accumulated in the photo-sites to the CCD analog shift registers. There are two transport CCD shift registers on each side of the linear array of photo-sites, outside of the transfer gate. Alternate charge packets are transferred to the CCD shift registers and then are transported serially to the output amplifier. Thus, the even and odd numbered pixels are transported in opposing CCD shift registers. The TC-103 has been physically and electrically designed to provide for alternate delivery of pixel charge packets to the output amplifier to re-establish the original sequence of linear image data. The output amplifier voltage varies linearly in response to the amount of signal charge delivered to it by each pixel. The maximum signal voltage corresponding to the white reference level is approximately 1 volt peak-to-peak.

Eight additional sensor elements, four at each end of the sensor array, are covered by opaque metallization. These elements provide a black reference signal, corresponding to zero accumulated charge. The black reference pixel information is output near the beginning and end of each transfer of linear array data from the CCD. Similarly, two pixels carry white or saturated reference level information in the output signal. These reference signals are output near the end of the output data sequence and are useful as inputs for external circuitry to provide d.c. restoration and automatic exposure control. Also included in the output train of analog signal levels are isolation pixel data levels, which do not contain meaningful information. A total of 2081 pixels are read out on each transfer of data from the CCD, but only 2048 pixels contain actual image data. The actual analog data pulse-train is illustrated in Figure 2.

A vertical cross-section of the TC-103 for two adjacent "pixels" is shown in Figure 3 with the mechanism for charge transfer illustrated in Figure 4. The VP CCD is a variation of the conventional buried-channel CCD. One layer of polysilicon gates are replaced with a heavily doped p-region near the silicon surface, which is known as a virtual electrode. A virtual barrier (VB) and well (VW) are created under the polysilicon gate by controlled doping of n-type implants. The electric field distributions in the virtual regions are independent of gate bias. The clocked electrode is fabricated similarly to a conventional two-phase CCD. A shallow, n-type implant under the clocked electrode forms a clocked well (CW) region and the remaining region of the clocked electrode forms the clocked barrier (CB). The electric field in the clocked regions can be controlled by manipulating the bias applied to the gate electrodes.

The combination of the clocked barrier/well and virtual barrier/well form the elementary structure of the CCD. During exposure, electrons accumulate in the potential wells due to particle events. After the exposure period has ended, the clocked electrodes transfer the charge by moving their corresponding potential wells above and below the levels of the virtual electrodes' barriers and wells. This is achieved by alternately clocking the gate potential from -15 volts to +4 volts. By repeating this process, the charge packets can initially be moved into the CCD transport channel from the photo-sites and then down the transport CCDs. The charge-transfer efficiency (CTE) of this device, which is the fraction of charge transferred from one well to the next, is approximately 0.99997 [23], for both the even and odd transport CCDs.

VP technology has resulted in improvements in device yields and performance over other CCD designs. The

elimination of one polysilicon gate results in higher device yields that are more efficient in front-side illumination, since less incident energy is absorbed by gate-electrode structures. Total dose effects (i.e. charge build-up in the $Si-SiO_2$ interface) can cause an offset in clock voltages and an increase in signal dark current. Through the simplification of the CCD gate clocking structure and since the charge transport occurs in a buried channel physically separated from the $Si-SiO_2$ interface, the VP CCD is more resistant to total dose-induced changes in device performance, such as decreased CTE and increased dark current.

3.0 EXPERIMENTAL SYSTEM

The commercially available TC-103 CCD was supplied with a glass window that was glued to the ceramic IC package. After some trial and error, it was found that the windows could be removed after heating the CCD to a temperature of 180-200 degrees Celsius for 10 minutes and prying the window off with a razor blade cutting tool. The CCDs were electrically tested after this procedure to ensure that the devices used for the experimental work were operational and within manufacturer's specifications.

A block diagram of the experimental apparatus is shown in Figure 5. It was desirable to use the DREO Van de Graaff Accelerator as a source of variable energy ions (i.e. protons and/or alpha particles) for this work, but was unavailable due to a shutdown for major equipment modifications. Furthermore, since the DREO Van de Graaff is limited to a 1-3 MeV energy range for single-charge positive ions, it was decided to use a higher energy monoenergetic alpha particle source mounted in a vacuum chamber instead. The energy of the alpha particles incident on the CCD could

then be controlled via the insertion of energy attenuating foils between the source and CCD or by the control of the degree of vacuum in the chamber. The energy-attenuation technique, however, has the undesirable effect of producing increased broadening of the energy spectrum of the alpha particles incident on the CCD. The greater the attenuation of the primary alpha particle energy, the larger the variation in the mean transmitted energy, due to the statistical variation in path length.

A bare 5.55 kBq ^{241}Am (Amersham no. AMR.13) source, emitting 5.48 MeV alpha particles was selected for use in this work. The source consisted of a very thin layer of ^{241}Am electro-deposited onto the central 7 mm diameter of a 25 mm diameter (0.5 mm thick) stainless steel disk. The energy degradation of the 5.48 MeV alpha particle emission, due to sample self-absorption, was certified by the manufacturer to be less than 20 keV, full-width at half-maximum (FWHM). The low activity of the alpha particle calibration source used in this work was of extreme importance to the experimental results. A small particle fluence was necessary to ensure that the soft error rates were also very low. This enabled the study of soft errors in isolation, i.e. in the absence of multiple alpha particle effects. The outcome of the experimental work would have been drastically different had a high flux source been utilized, such as has been used in other's work [21].

A commercial 8 bit, 25 MHz (maximum) sampling rate, PC-based flash analog-to-digital converter (ADC) was used to digitize the pixel data from the CCD. External circuitry was required to provide synchronization between the CCD and ADC clock signals as well as to synchronize data acquisition with the start of each transfer of data from the CCD. Since the CCD signal range was between 7 and 8 volts d.c., a

200 MHz d.c. coupled amplifier was used to adjust the signal level to the 0-1V input range of the ADC and to provide a small signal gain (1 to 5) if required.

The CCD pixel data transfer rate used was 700 kHz and the exposure duration was 10 ms. Longer exposures could have been used, but at the expense of a larger dark current, due to thermally generated carriers in the CCD. The data transfer rate was controlled by the signal RCK and the exposure duration was controlled by XCK (see Figures 2 and 5) After a single frame of information was acquired by the ADC (i.e. 2048 image pixels and reference pixels), the data was transferred from the ADC's buffer to the PC's memory by direct memory access (DMA), for maximum transfer speed. The data acquisition system and software used for these experiments, as well as CCD clocking frequencies, limited the data acquisition live-time to approximately 8-10%.

A digital discriminator level was set via software to select valid particle/pixel events. The discriminator level was adjusted to provide minimum false event triggering due to CCD and electronic system noise. When a valid event was detected, the run number (i.e. how many "frames" of 2048+reference level pixels have been read), pixel number and corresponding pulse-height data were recorded on the PC's hard disk. Also recorded were data for several pixels on either side of the hit pixel, even if their corresponding pulse-heights were below threshold. The pulse-height for the two white reference pixels and four black reference pixels were also stored for frames of data that had one or more valid events. The reference pixel data was stored to provide an off-line method of providing accurate d.c. restoration of the pixel pulse-heights and to monitor the dynamic range (e.g. signal gain) of signal pulse-height.

The CCD was operated at room temperature, in total darkness, in a vacuum chamber with an absolute pressure less than 0.1 mm Hg. The CCD-source geometry and distance could be easily varied in a reproducible manner. The CCD was subjected to alpha particles over the entire die of the device and over the central 10% of the array by the use of a removable metal shield with a small slit in it. The 127 μm thick tin shield was impenetrable by 5.48 MeV alpha particles (range=18 μm, calculated using TRIM).

4.0 EXPERIMENTAL RESULTS

4.1 ALPHA PARTICLE IRRADIATION OF THE ENTIRE CCD ARRAY

The TC-103 CCD was found to be very sensitive to the 5.48 MeV alpha particles and produced a signal with a substantial signal-to-noise-ratio (SNR), clearly distinguishable from background noise. No reduction in the amount of vacuum, to attempt to increase the dE/dx of the alpha particles as they traverse the sensitive charge collection volumes within the CCD, was required to produce a detectable signal. Since Texas Instruments would not supply information regarding the depth and width of the charge collection region, varying the vacuum was to be an alternate approach to increase the dE/dx of the alpha particles in the device, if a poor SNR was obtained. Typical output waveforms for various types of single alpha particle pixel hits are shown in Figure 6.

A typical alpha particle energy spectrum was obtained from the CCD (Figure 7) by methods similar to those used in previous investigations by others [21, 22]. The duration of the experimental run was 89.2 hours and during this time interval, 2,570,022 frames of CCD data were digitized. Any pixel in the CCD array that produced an output signal that was above the digital discrimination level was treated as a

valid isolated single-event and the pulse-height was accordingly scored.

The data consists of a single poorly resolved peak (approximately channel number 120), corresponding to the most-probable maximum energy imparted by the 5.48 Mev alpha particles. The "background" rapidly increases from the peak to lower channels. The digital discriminator level was set to channel 40, therefore, no counts were recorded below this. The average black and white reference pixel pulse-heights for the entire run were 17 and 176, respectively (1 channel=3.92 mV). In previous work [21, 22], it was assumed that the energy spectra obtained were from single pixel alpha particle hits, i.e. a single alpha particle traverses the sensitive volume of a single photo-site.

In this work, more detailed analysis could be performed (at a later time) because, as previously mentioned, data regarding each pixel hit and other bookkeeping information was sequentially stored to disk. Before presenting the results of further analysis, definition of different types of pixel hits are required. The methodology for classification of different types of pixel hits is summarized in Table 1. Pixel hits (denoted by '*') detected during the sequential read-out of a single frame of CCD data are classified and sorted according to the linear sequence of pixel hits and background (denoted by 'b') pixels encountered.

It should be noted that multiple alpha particle hit sequences are not included in Table 1 because of the extremely small probability of occurrence. At a typical source-CCD distance of 5 cm, with the source directly above the middle of the linear CCD array, the flux of alpha particles (assuming a point source) from the ^{241}Am source

PIXEL SEQUENCE	HIT DESIGNATION
b-b-*-b-b	single pixel hit
b-b-*-*-b-b	single adjacent pixel hit
b-b-*-b-*-b-b	single transport CCD hit
b-b-*-*-*-b-b-b	single triple pixel hit
b-b-*-*-*-*-b-b	single quadruple pixel hit
etc.	etc.

Table 1. Classification of the type of pixel hit by output pixel sequences from CCD. These event sequences are caused by a single alpha particle interaction in the CCD.

would be 17.7 $s^{-1}cm^{-2}$ in the middle of the array (decreasing to 16.6 $s^{-1}cm^{-2}$ at opposite ends of the array). The pixel size was 12.7 microns on each side (square), therefore, the alpha particle flux per pixel was $2.85 \times 10^{-5} s^{-1}$ in the centre of the array. Over a 10 ms exposure period, the probability for a single pixel hit, assuming 100% detection efficiency, was 2.85×10^{-7}.

Since the statistics of alpha particle emission (radioactive decay) is governed by Poisson statistics, the probability for emission of two alpha particles from the ^{241}Am source within the 10 ms exposure period can be determined. The probability of observing n counts in the time interval t when the average counting rate is r (observed over a long time interval), is given by $P_n=((rt)^n/n!)\exp(-rt)$. The probability of emission for n=2 alpha particles within the 10 ms exposure time, for a rate $r=5.55$ kBq$=5.55 \times 10^3 s^{-1}$ is, therefore, $P_2=1.21 \times 10^{-21}$. It is readily apparent that, after taking into account the solid angle, the probability for two separate alpha interactions in two pixels during a single 10 ms exposure is highly improbable ($P<9.83 \times 10^{-35}$).

Figure 8 shows only the single isolated single pixel hits from the previous data. A significant improvement in

resolution is observed, with a corresponding decrease in the integral number of particle events.

Figure 9 shows an energy spectrum of single pixel hits for which the pixel pulse-heights have been d.c. restored (to zero d.c. bias) and partially corrected for charge transfer inefficiency (CTI=1-CTE). Finite time interval averages (e.g. 500 consecutive frames of CCD) of the black reference pixels were subtracted from the corresponding pulse-height data to obtain zero d.c. bias corrected pulse-height data. The difference between time-averaged white and black reference pixel data was used to monitor the electronic system's gain. Since the CTE is slightly less than unity in CCDs, some charge leaks from one pixel to another during transfer and show up as low level (below the discriminator level but above the black reference level) "noise". The single hit data was corrected for CTI by addition of the pulse-height of the single "background" pixel immediately following it. This procedure resulted in a significant improvement in energy resolution.

The single hit pulse-height data has been separated into even and odd pixels data in Figure 9. A slight difference in pulse-height spectra for even and odd pixels was observed during short duration experiments (<8 hrs). This difference is attributed to slight physical and electrical differences between the even and odd transport CCDs, which is consistent with the manufacturer's data sheet specification of a maximum "alternate register imbalance" of 10 mV. In experiments of longer duration, the odd/even pixel imbalance was masked due to temperature-induced gain shifts in the CCD and amplifier electronics. The electronics system was operated at ambient temperature which fluctuated by as much as 10 degrees Celsius during a 24 hour period. In this work, the register imbalance was measured

using an oscilloscope, to observe the differences in signal level between even and odd reference pixel levels. For the data presented in Figure 9, the difference in the average black reference pixels for even and odd pixels was typically 9.5 mV. The difference in the white reference pixels for even and odd numbered pixels was typically 10.0 mV. It should be noted that this measurement was performed on only 1 CCD. Other TC-103 devices may exhibit different (i.e. possibly better) performance.

The spatial distribution of single pixel alpha particle hits over the entire (1 inch long) linear array is shown in Figure 10. This data is for the same pulse-height data presented in Figure 9. As expected, the middle of the array recorded the greatest number of hits per channel due to the smallest source-detector distance. Since the ends of the arrays are further away from the source the alpha particle flux is reduced according to the inverse-square law. The alpha particles strike the CCDs surface at increasing angles of incidence toward the ends of the arrays and, therefore, the effective surface area of the target decreases. Analysis could not be performed to fully quantify this effect as the required device data, such as depletion depth and width, could not be obtained from the manufacturer.

The pulse-height distribution for adjacent pixel hits that has been d.c. offset corrected and partially corrected for CTI is shown in Figure 11. Separate pulse-height distributions for even and odd pixels are also included. A broader distribution in pulse-height than that for single pixel hits was observed and can be qualitatively explained in terms of the statistical nature of the energy deposition and charge creation/collection process. What is of note, however, is that the mode of the distribution occurs approximately at the same location as that for single pixel

hits. Although it is not conclusive proof, it is a good indication that the energy deposition and charge collection occurred under the same conditions, e.g. in the same thickness, type and depth of material, as for the single pixel hits.

The pulse-height distribution for transport CCD pixel hits that has been d.c. offset corrected and partially corrected for CTI is shown in Figure 12. Separate pulse-height distributions for even and odd pixels are also included. The mode of the pulse-height distribution occurs at a higher channel number than that for single pixel and adjacent pixel hits. This and other arguments, to be presented, support the observation that these events are due to single alpha particle hits on the transport CCDs and not on the photo-sites. There is no reasonable argument that a single alpha particle could cause a large signal level in two pixels separated by a "background" pixel in the linear photo-site array. Statistical arguments presented have indicated that it is very improbable that multiple particles caused these events, especially when the relative frequency of events presented in Table 2 are considered.

TYPE OF PIXEL EVENT	NUMBER OF EVENTS	PERCENT OF TOTAL EVENTS
single pixel hits	67,675	66.7
transport CCD pixel hits	20,837	20.5
adjacent pixel hits	12,884	12.7
other pixel hits	103	0.1
TOTAL NUMBER OF EVENTS	101,499	100.0

Table 2. Relative occurrence of single, adjacent, transport CCD and "other" types of pixel hits for data presented in Figures 9 through 13.

From Table 2, pixel hits in the transport CCDs represented 20.5% of the total number of pixel events detected. As has already been demonstrated, the probability of these events occurring due to multiple alpha particle hits in the linear array of photo-sites is extremely small. [If the area, depletion width etc. of the transfer wells and photo-sites was known, the relative number of expected hits for single, transport CCD and adjacent pixel hits could be analytically determined]. The only physical location in the CCD where charge packet numbers 'n' and 'n+2' come into close proximity, i.e. when they are physically adjacent to each other, is in the transport CCDs. During a 10 ms exposure interval, the transport CCDs contain valid pixel data that is being shifted towards the charge sensitive amplifier for approximately 3 ms (2081 pixels are transferred at a 700 kHz pixel transfer clock rate). In the other 7 ms, it is not known from TI's data sheets if the transport CCDs are clocked or static, although several physical arguments support reasoning for continuously clocked transport CCDs. The uniform spatial distribution of transport CCD pixel hits (Figure 13) suggests that the transport CCDs are clocked. With the exposure duration and pixel transfer rates used in this work, the transport CCDs would have to be continuously clocked to achieve the uniform distribution shown in Figure 13. The results of the next section, in which the CCD was masked except for a narrow slit in the middle of the array, will conclusively verify the occurrence of transport CCD pixel hits and the continuously clocked transport CCDs.

From Table 2, the total number of events was 101,499, which implies that the same number of alpha particles hit SEU-sensitive regions of the CCD. From the pulse-height spectrum for the unprocessed data of Figure 7, the integral counts indicate that a total of 138,022 alpha particles were incident on the array. The latter value, if used to infer

SEU sensitivity of the photo-sites or detector efficiency, leads to erroneous conclusions.

4.2 SINGLE SLIT EXPERIMENT

Since only approximately the central 10% of the linear CCD array was exposed to alpha particles, the source-CCD distance was reduced to approximately 0.5 cm to achieve higher count rates. This significantly increased the solid angle between the source and CCD compared to the previous experiment. Thus, broadening of the alpha particle energy distribution might be expected, due to a potentially greater variation of alpha particle path lengths. The pulse-height distribution for single pixel hits, (Figure 14) supports this assumption. If the alpha particle completely traverses the "charge collection volume" of a pixel, then the alpha particle's path length would vary as $\sec(\theta)$ where θ is the angle of incidence with the CCD's surface. If the pixel is not saturated by the traversal of an ion then geometry effects could result in a larger pulse-height. The pulse-height distribution of Figure 14 reflects this phenomena when compared to the distribution of Figure 9, where the solid angle was much smaller. In Figure 14, a portion of the spectrum has been redistributed to higher pulse-height.

The spatial distribution of single hits, adjacent hits and transport CCD pixel hits, for the single slit experiment, are shown in Figures 15 through 17, respectively. The single hit spatial distribution shows a peak in the middle of the array corresponding to the slit opening, but also shows a relatively uniform "background" extending throughout the remainder of the array. It is impossible for the alpha particles to penetrate the tin shield, since the range of the alpha particles are much less than the thickness of tin used. To test the hypothesis that

the 59.5 keV x-ray that is also emitted during the radioactive decay of ^{241}Am was not the cause of the pixel hits, the following simple experiment was performed.

The source-CCD distance was set at 5 cm, the slit was removed to optimize detection efficiency and the vacuum chamber was operated at atmospheric pressure. In 5 cm of air at 760 mm Hg (1 atmosphere), the range of 5.48 MeV alpha particles was calculated (using TRIM) to be 4.22 cm with 0.17 cm straggle. Therefore, the CCD was adequately beyond the range of the alpha particles. However, the 59.5 keV x-ray can penetrate 5 cm of air with little attenuation (μ_a/ρ=.0188 g cm^{-2} for 60 keV photons [29]) and interact with the CCD. No events above the discriminator level were detected. This verifies the hypothesis that the 59.5 keV x-rays were not responsible for the pixel hits. For interest sake, this was repeated for a 1 μCi ^{60}Co source (1.25 MeV average gamma-ray energy). Again, no events above the discriminator level were detected.

The probable explanation for the background events observed in Figure 15 is that the events were caused by single pixel hits in the transport CCDs. From the graph of spatial distribution of adjacent pixel hits (Figure 16), it can be seen that no adjacent pixel hits occurred outside of the slit region. By definition, an adjacent even and an odd pixel have to be hit in order to be categorized as an adjacent pixel hit. It is impossible for this to occur in the transport CCDs, since even and odd numbered pixels are never in the same transport CCD.

The spatial distribution of pixel events for the transport CCDs (Figure 17) also confirmed that soft errors were introduced via the transport CCDs. An uniform distribution of events with respect to pixel number implies

that the transport CCD channel hits occurred as the empty transport CCD "pixels" were scanned through the slit. The uniform distribution of events also indicated that the transport CCDs were continuously clocked. Without clocking the transport CCDs, pixels corresponding to the vicinity of the slit opening would exhibit a higher percentage of the total number of events measured. A uniform background of events would appear for pixel numbers that are grater than that for the slit opening region, since these pixels would be transported past the slit opening, at a uniform rate.

It is interesting to note that transport CCD pixel "hits" are not introduced by optical (i.e. visible) radiation in more traditional applications of CCDs. This is most likely due to the transport CCDs being covered by metallization to make them opaque to eV range photons, although we have substantiated this. The 5.48 MeV alpha particles are capable of penetrating Al metallization of several microns without significant energy loss.

5.0 CONCLUSIONS

The mechanisms for generation of single-event upsets were studied in the TC-103 linear array CCD. A new mechanism for the induction of SEUs in this CCD - alpha particle hits in the transport CCDs, has been experimentally demonstrated. This phenomena may have deleterious consequences for applications employing CCDs as position-sensitive ionizing radiation detectors because of the possibility of having soft errors or data artifacts introduced into spatial domain data. CCD detectors are currently being designed and employed for detection of ionizing radiation ranging from low energy x-rays to high energy particles produced via nuclear reactions. The

integrity of spatial and energy information is usually of paramount importance. In these applications, low flux sources should be used to characterize the CCD in a similar fashion to the procedure used in this work, in order to evaluate the suitability of a particular CCD.

In order to improve the live-time performance of our data acquisition system, a dedicated microprocessor-based ADC and control system is required. The system should be able to perform spatial correlation of pixel data ("cluster" analysis) in real-time. Such a system is being designed and built for future experimental work to be conducted at DREO. It is also desirable to extend this work to 2-dimensional arrays and to investigate other CCD architectures.

Spatial correlation or cluster analysis techniques used in analyzing single-event induced pulse-height data are essential to characterize mechanisms of SEU error generation in CCDs and other matrix-type devices (such as digital memory devices) that are susceptible to SEUs. A variety of different types of single-event phenomena have been demonstrated in the TC-103 CCD. The indiscriminate use of raw pulse-height data can lead to errors in the estimate of SEU sensitivity of integrated circuit designs, if soft errors are attributed to the wrong circuit components. The techniques used in this work for the experimental evaluation of CCDs can also lead to a greater understanding of the physics and operation of these devices.

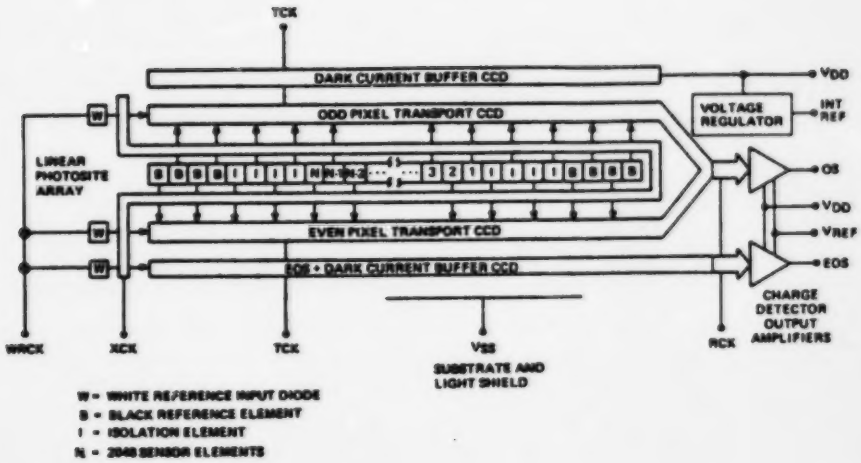

SIGNATURE	NAME	DESCRIPTION
V_{REF}	Reference Voltage	Bias input for the output amplifiers and internal reference.
OS	Output Signal	Video output from a cascaded source-follower MOS amplifier.
V_{DD}	Supply Voltage	Output amplifier supply voltage.
V_{SS}	Substrate	All voltages are referenced to the substrate.
INT REF	Internal Reference	Potential derived internally for operational reference voltage.
NC		No internal connection.
TCK	Transport Clock	Drives the CCD transport registers.
WRCK	White Reference Clock	Injects a controlled charge into the white reference CCD shift register elements to become white-reference and end-of-scan pulses.
XCK	Transfer Clock	Controls the transfer of charge packets from sensor elements to shift registers. The interval between pulses of the transfer clock determines the exposure time.
RCK	Reset Clock	Controls recharging of the charge-detection diodes in the output amplifiers, and clocks the output shift registers where the odd and even signals have been merged.
EOS	End-of-Scan Pulse	Indicates that all charge packets have been shifted out of the transport registers.

Figure 1. Functional block diagram of the Texas Instruments TC-103 2048 element, virtual phase charge-coupled device.

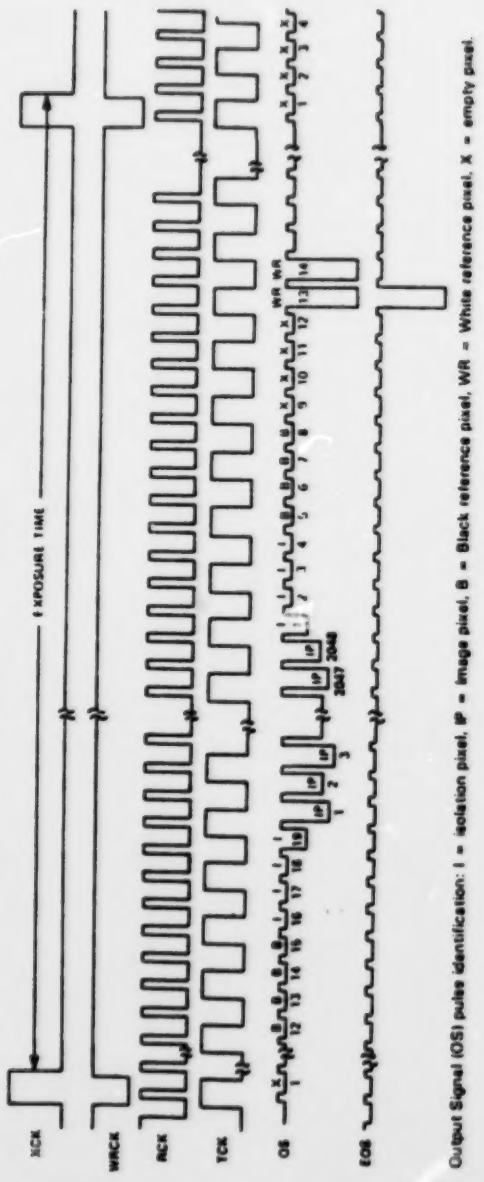
EXPOSURE TIME
XCK
WRCK
RCK
TCK
OS
EOS
Output Signal (OS) pulse identification: I = isolation pixel, IP = image pixel, B = Black reference pixel, WR = White reference pixel, X = empty pixel.

Figure 2. Operating input and output waveforms for the Texas Instruments TC-103 CCD.

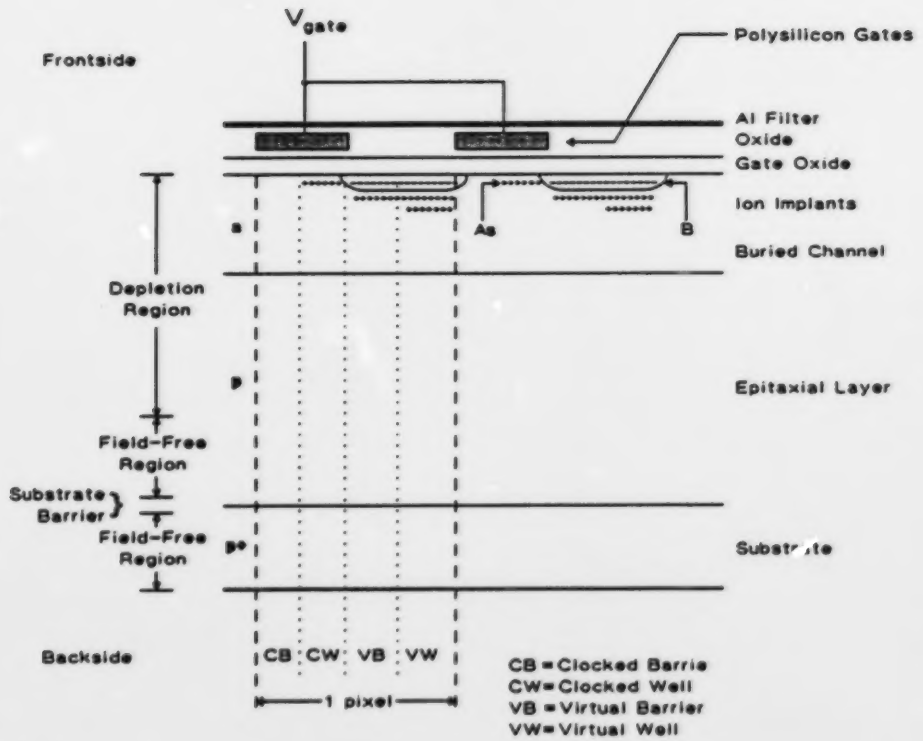

Figure 3. A vertical cross-section of the TC-103 CCD in the vicinity of two adjacent pixels. The clocked and virtual well/barrier regions are indicated for one pixel.

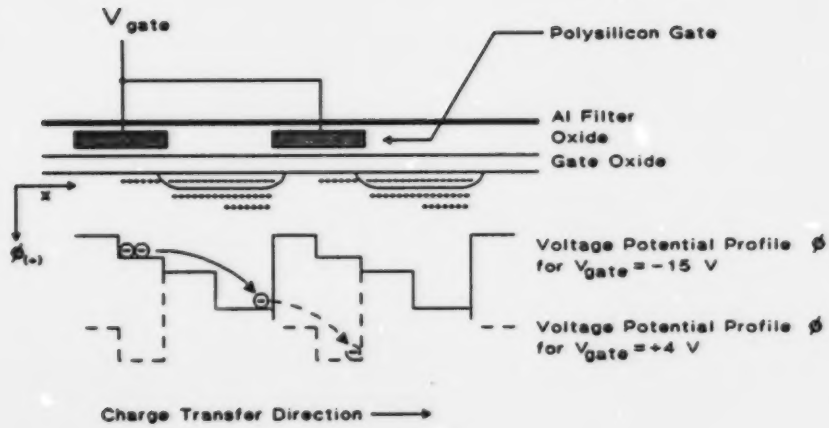

Figure 4. Illustration of the mechanism used to linearly transfer charge in the TC-103 virtual phase CCD. The voltage potential profile (ϕ) in the virtual barrier/well regions is not influenced by the gate potential.

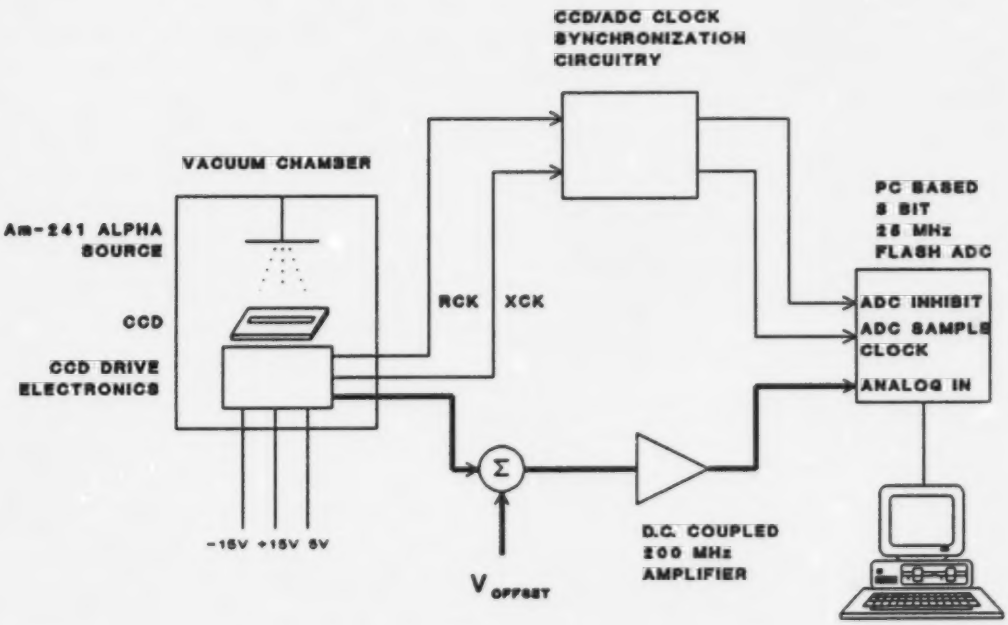

Figure 5. Block diagram of the experimental system employed in this work to investigate alpha particle induced SEUs in the TC-103 CCD.

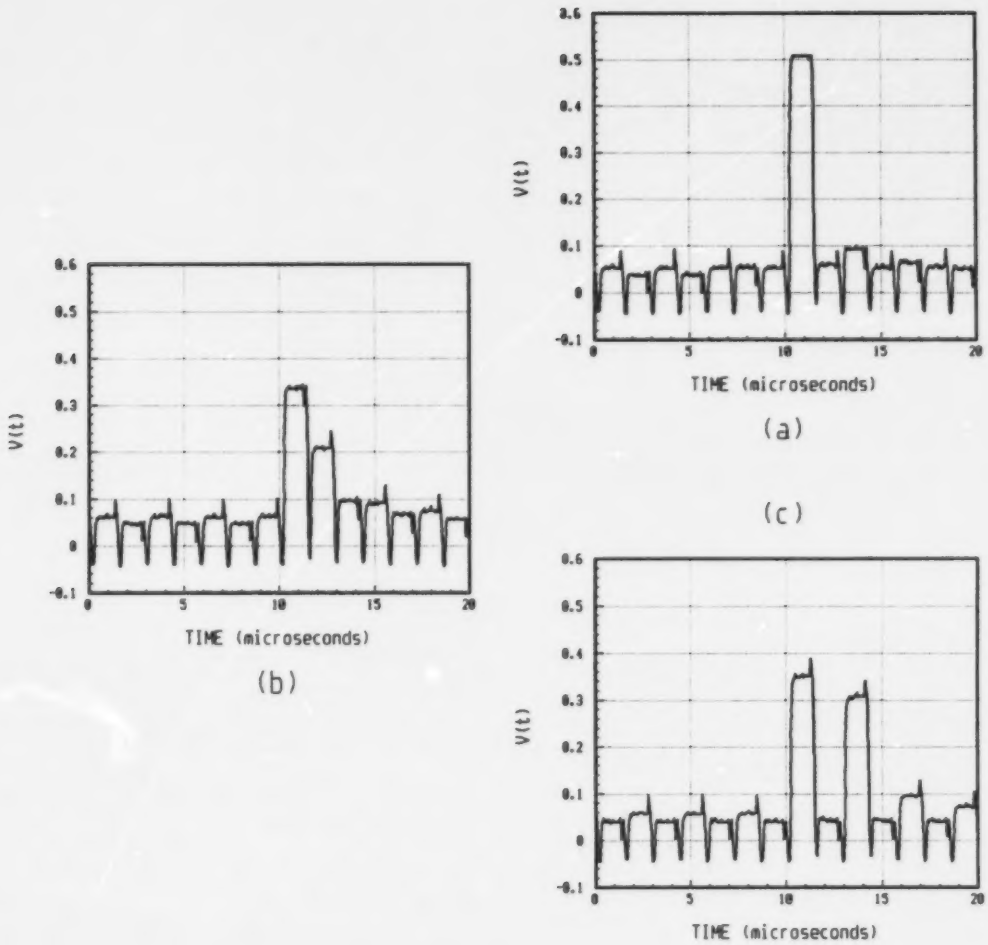

Figure 6. Typical output waveforms from the TC-103 CCD, captured by a 300 MHz digital oscilloscope, for a single alpha particle induced a) single pixel hit, b) hit on an adjacent pair of pixels and c) transport CCD pixel hit. The different types of pixel hits are explained in the text.

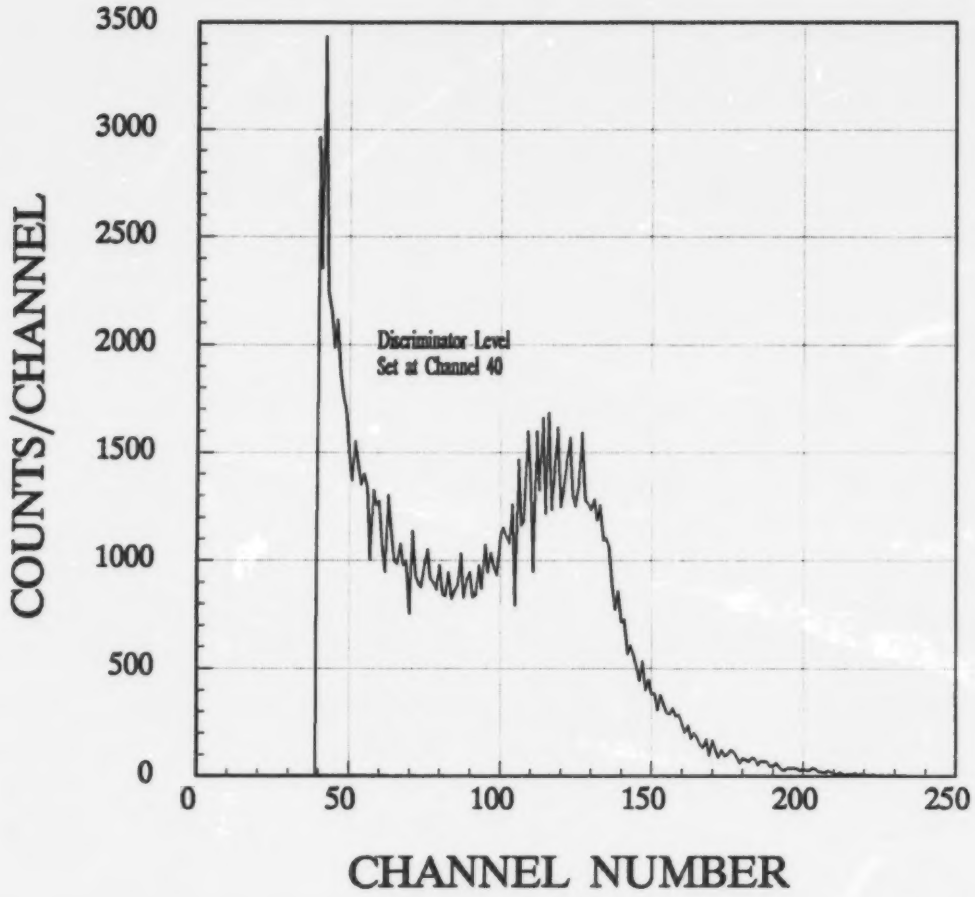

Figure 7. A typical "raw" pulse-height spectrum obtained for alpha particle induced SEUs in the TC-103 CCD. No data processing (e.g. spatial correlation or "cluster analysis") was performed on the raw data. The integral number of events recorded in the spectrum was 138,022.

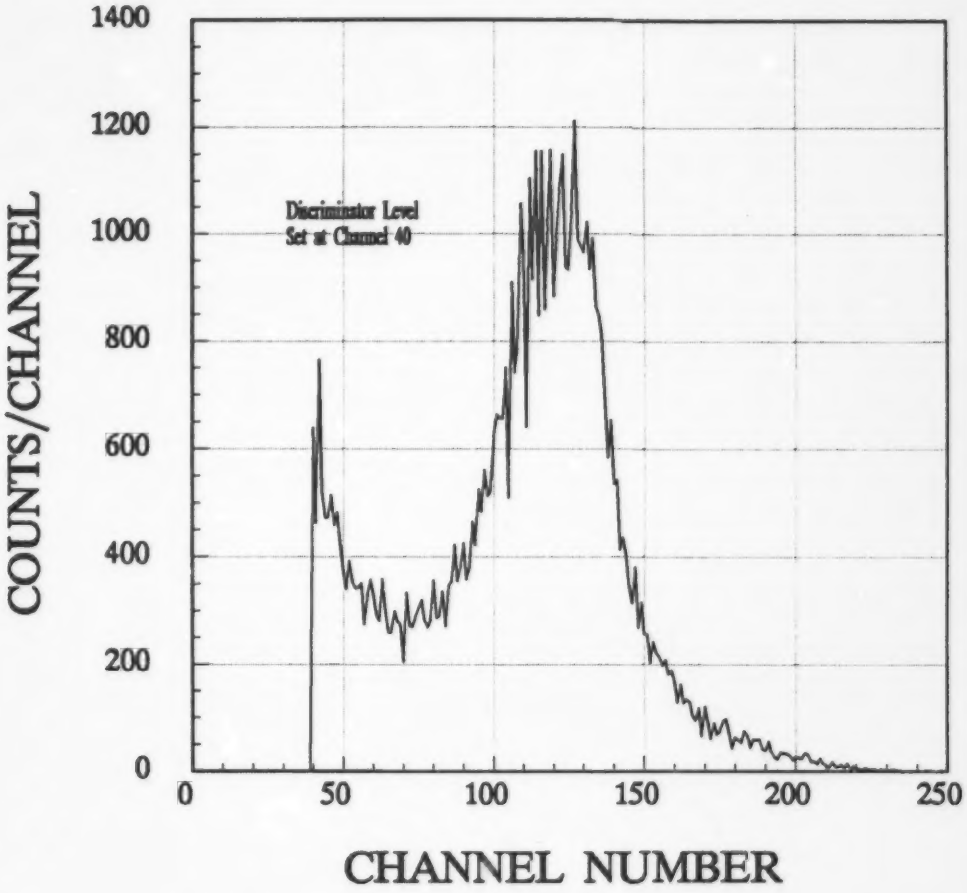

Figure 8. A pulse-height spectrum of isolated single pixel hits. This is for the same experimental run as presented in Figure 7. The integral number of events recorded in the spectrum was 67,675.

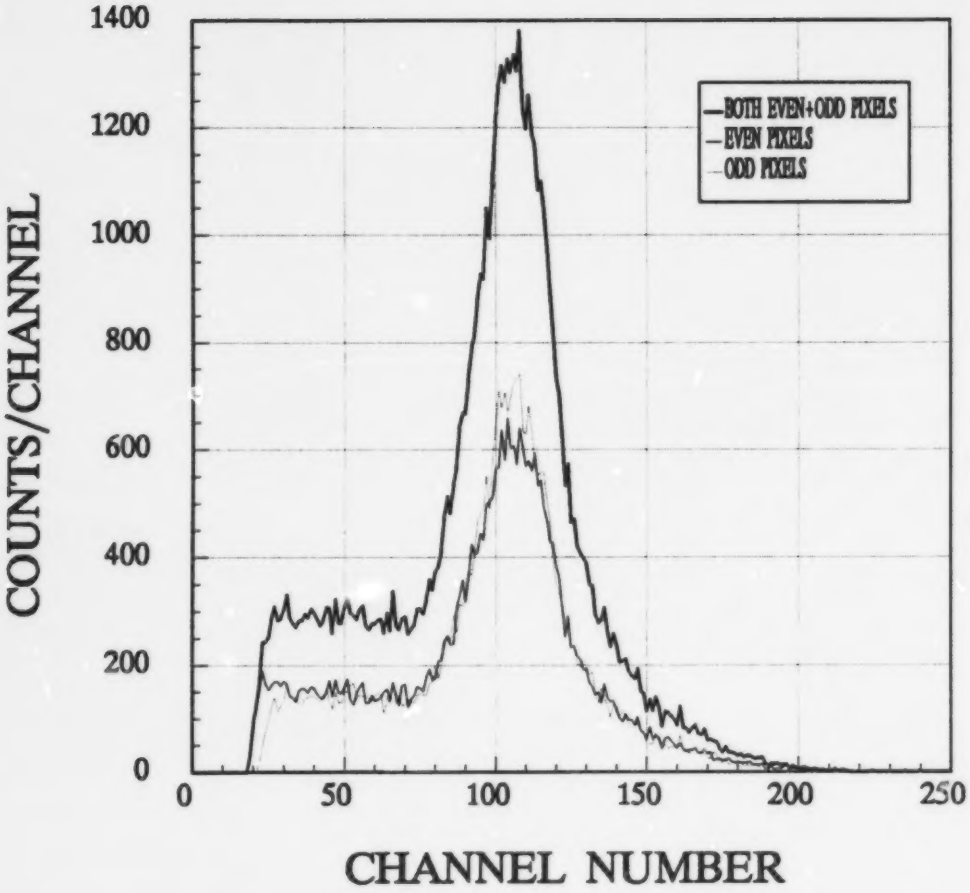

Figure 9. The same experimental data as in Figure 8, but the pulse-height spectrum of single pixel hits have been corrected for d.c. offset and charge transfer inefficiency (CTI), resulting in improved resolution of the peak. The pulse-height for even and odd pixels is also shown. The integral number of counts recorded in the spectrum was 67,675 (33,876 even pixel hits+33,779 odd pixel hits).

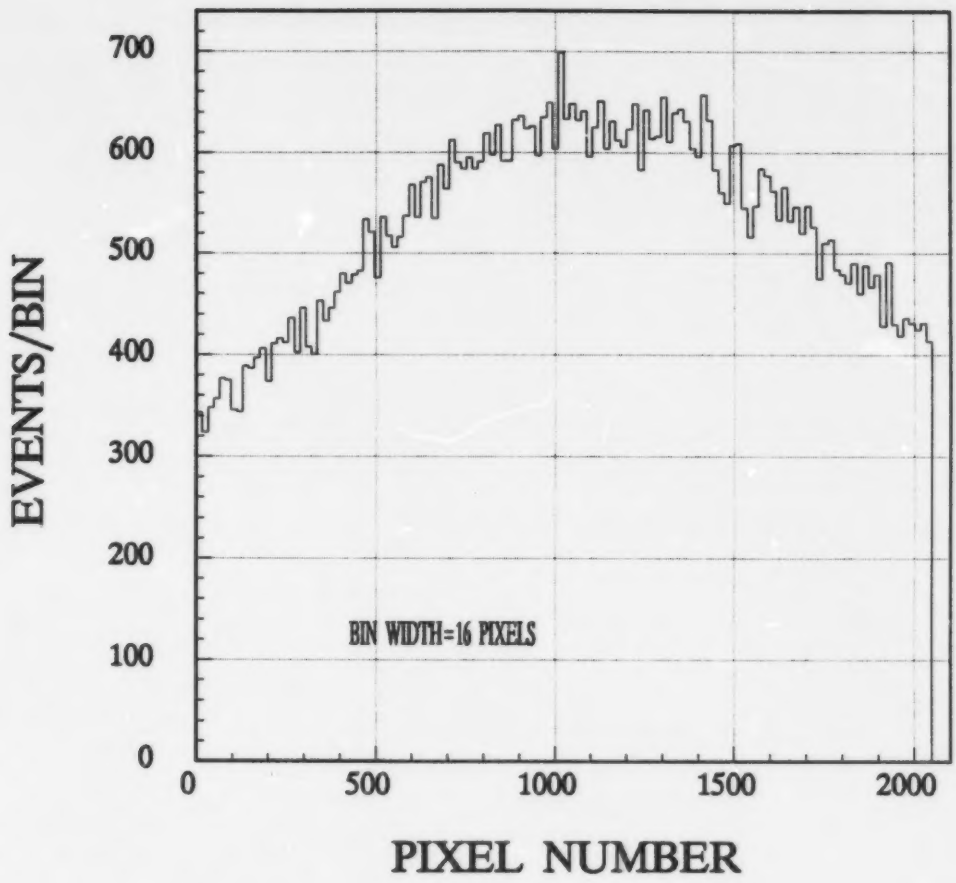

Figure 10. Spatial distribution of single pixel alpha particle hits for the data presented in Figure 9. The distribution is peaked towards the middle of the array due to differences in source-pixel solid angles. The "point" source was located directly above the linear array, near the centre.

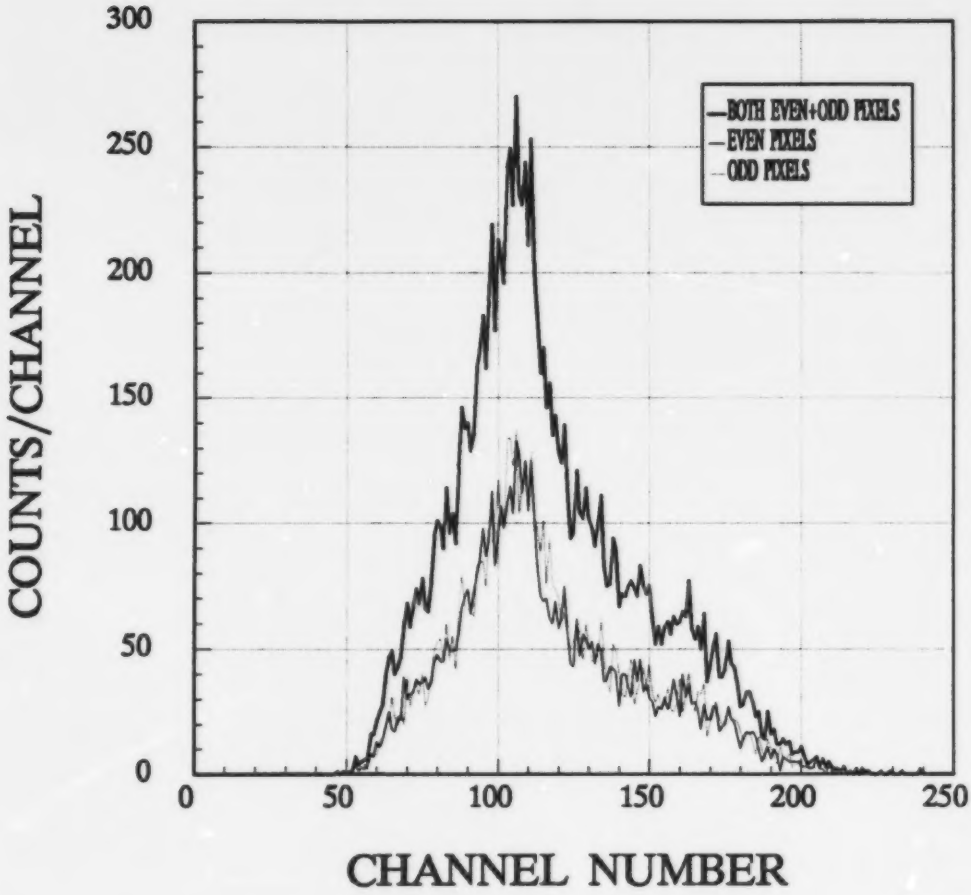

Figure 11. A pulse-height distribution for alpha particle induced adjacent pixel hits. The pulse-height shown represents the summed pulse-height of each even/odd pixel pair that forms an adjacent pixel hit. The data is for the same experimental run as in previous Figures and has been corrected for d.c. offset and CTI. Even and odd pixel pulse-height distributions are also shown. The integral number of events recorded in the spectrum is 12,884 (6,308 even pixels had the larger pulse-height of the even/odd pixel pairs and 6,576 odd pixel had the larger pulse-height of the even/odd pixel pairs).

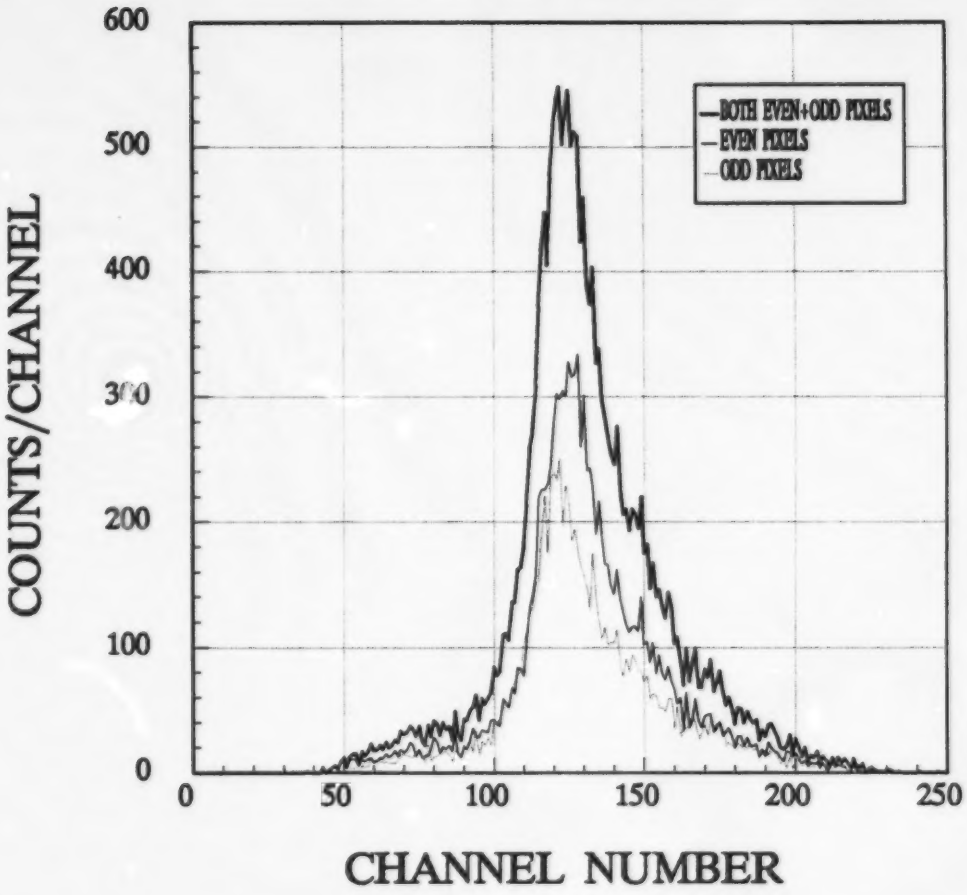

Figure 12. A pulse-height distribution for alpha particle induced transport CCD pixel hits. The pulse-height shown represents the summed pulse-height of each 2 pixels (i.e. pixel 'n' and pixel 'n+2') that form a transport CCD pixel hit. The data is for the same experimental run as in previous Figures and has been corrected for d.c. offset and CTI. Even and odd pixel pulse-height distributions are also shown. The integral number of events recorded in the spectrum is 20,837 (6,308 even pixels had the larger pulse-height of the even/odd pixel pairs and 6,576 odd pixel had the larger pulse-height of the even/odd pixel pairs).

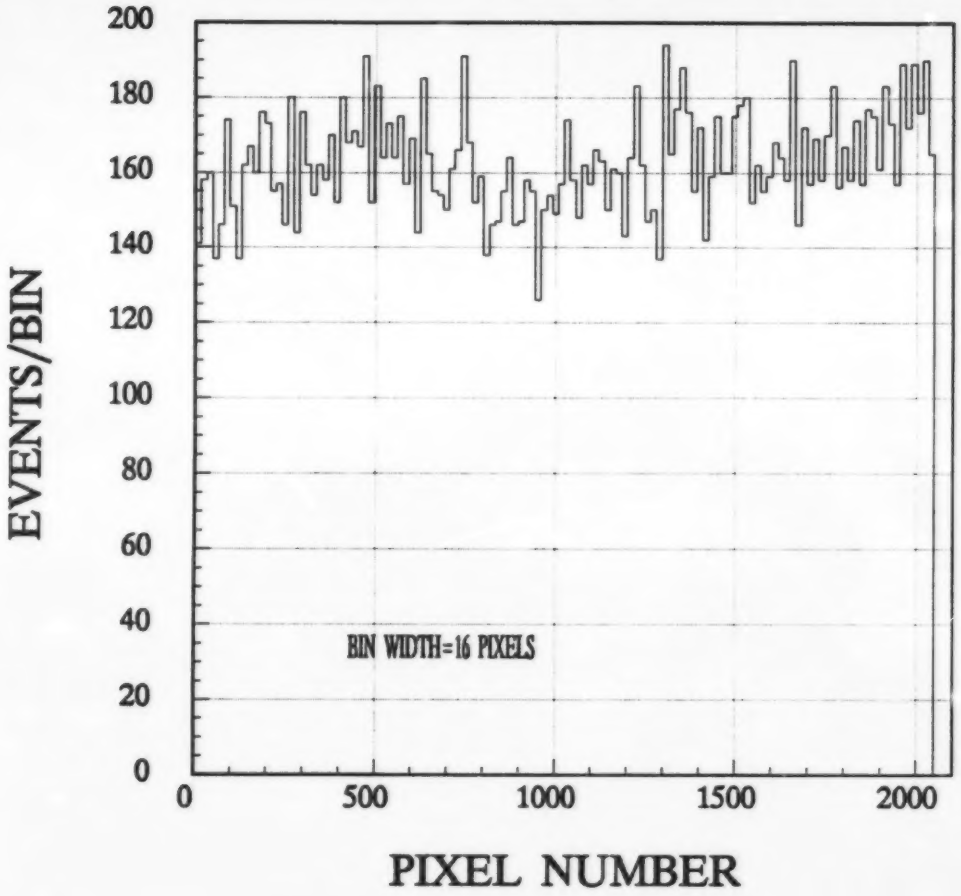

Figure 13. Spatial distribution of transport CCD pixel hits for the same data presented in Figure 12.

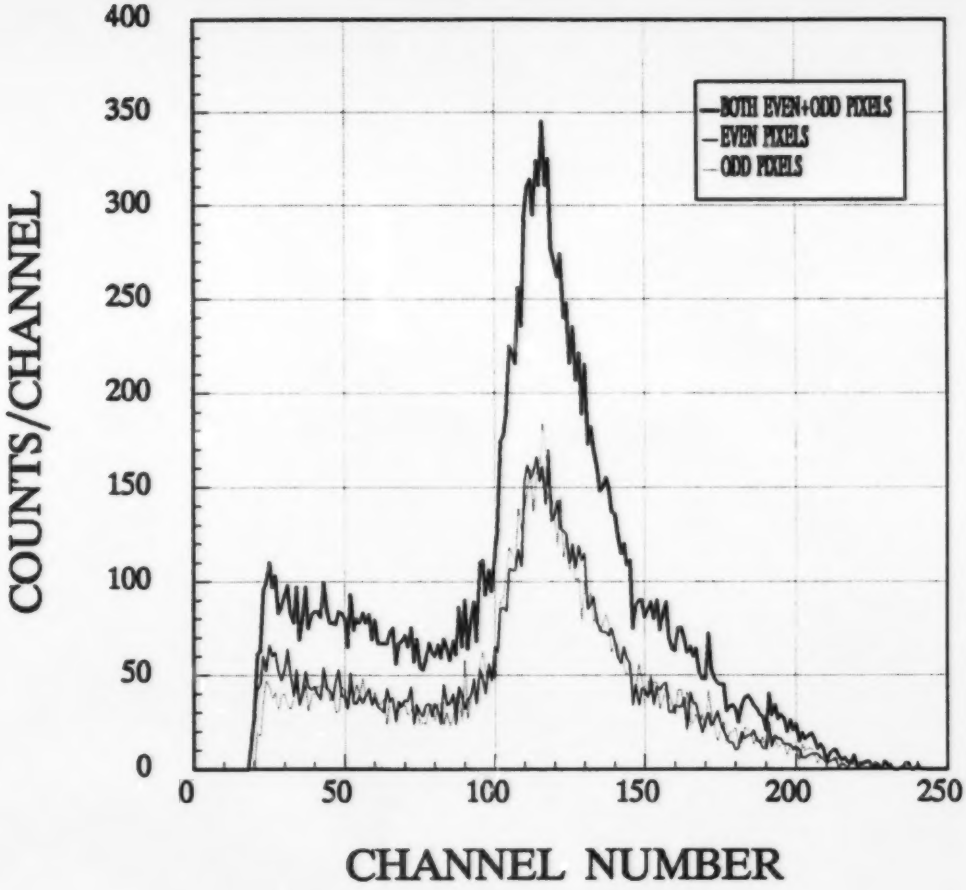

Figure 14. A pulse-height spectrum of alpha particle induced single pixel hits for the TC-103 CCD that has been covered, except for a narrow slit opening in the middle of the array. The 5.48 MeV alpha particles have insufficient energy to penetrate the thickness of the metal shield used. The data has been corrected for d.c. offset and charge transfer inefficiency (CTI). The pulse-height for even and odd pixels is also shown.

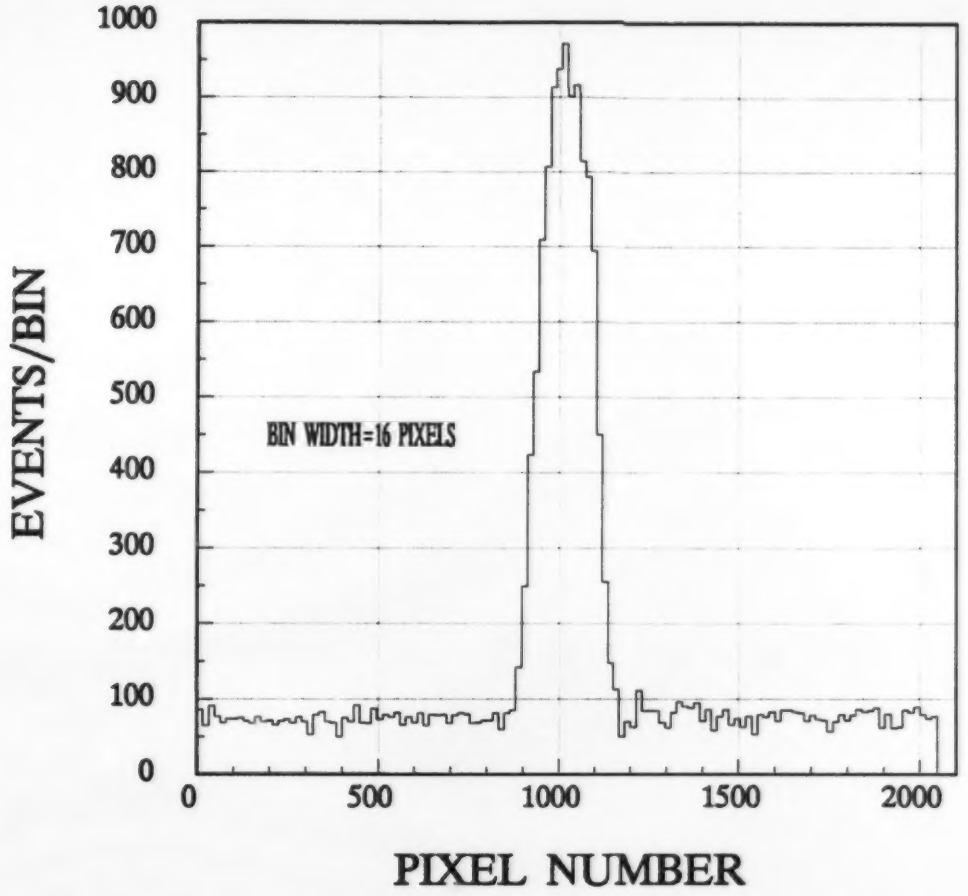

Figure 15. Spatial distribution of alpha particle induced single pixel hits for the narrow single slit experiment. The data is from the same experimental run as for the data presented in Figure 14.

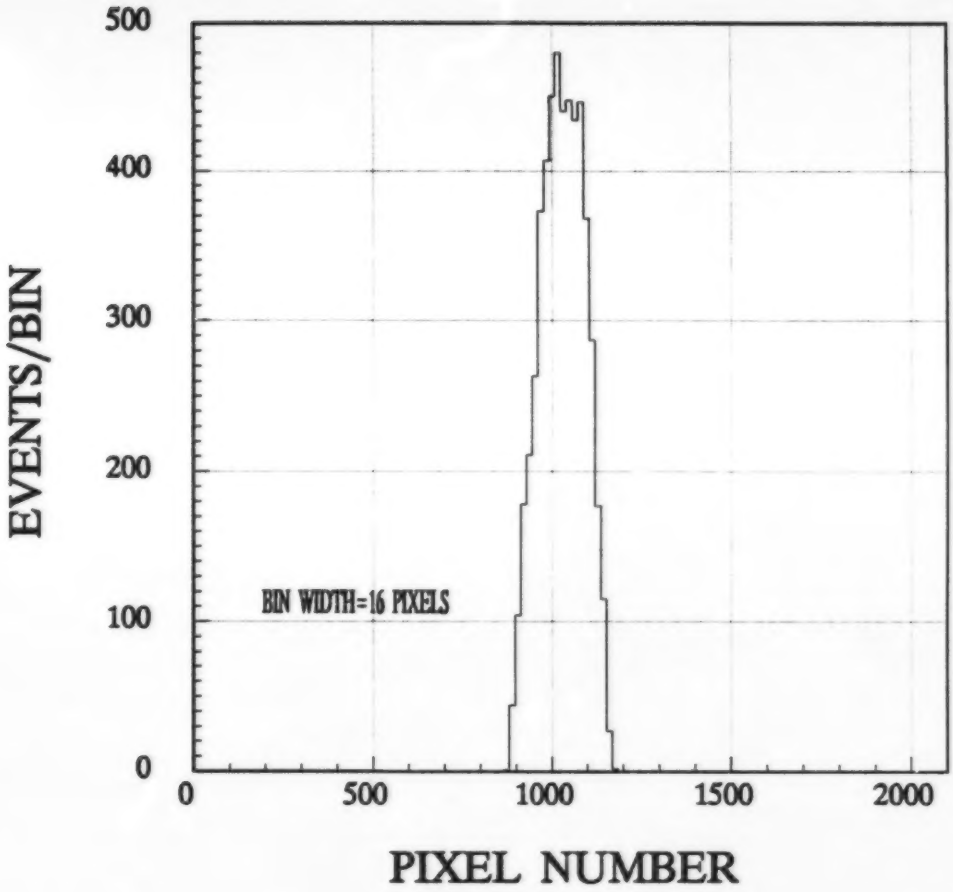

Figure 16. Spatial distribution of alpha particle induced adjacent pixel hits for the narrow single slit experiment. The data is from the same experimental run as for the data presented in Figure 14.

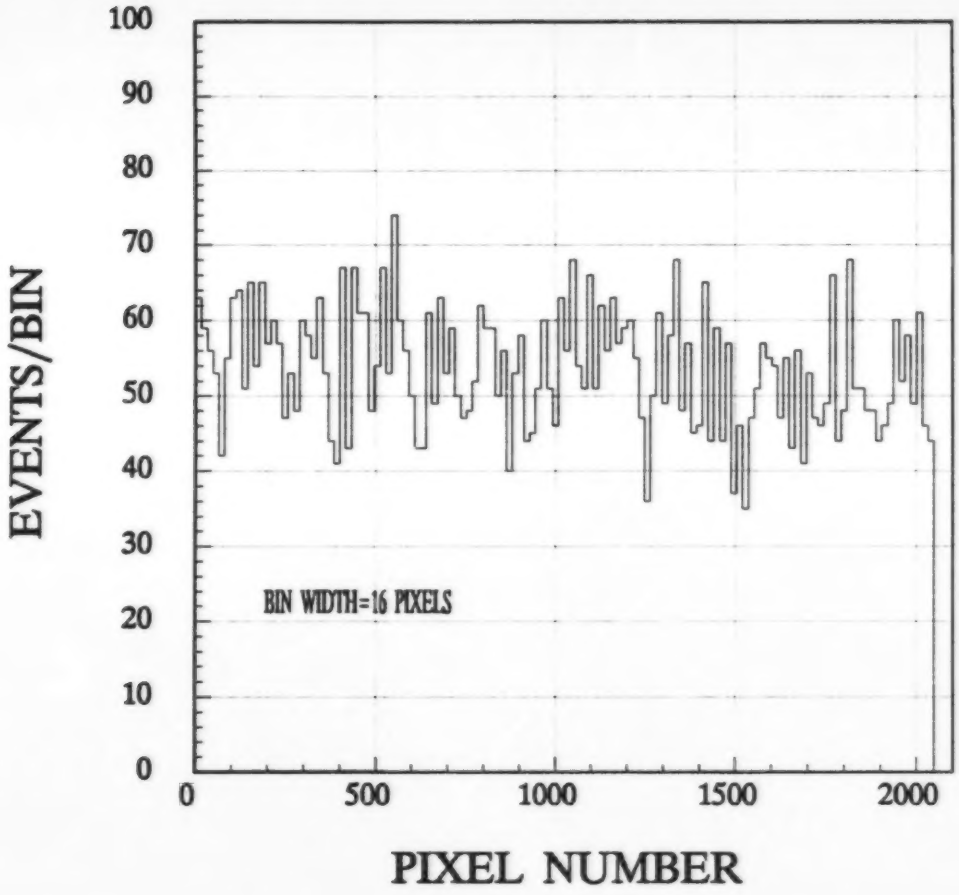

Figure 17. Spatial distribution of alpha particle induced transport CCD pixel hits for the narrow single slit experiment. The data is from the same experimental run as for the data presented in Figure 14.

REFERENCES

1. W. Boyle and G. Smith, "Charged Coupled Semiconductor Devices", Bell Syst. Tech. J. 49, 587-593 (1970).

2. J.R. Janesick, T. Elliot, S. Collins, M.M. Blouke, J. Freeman, "Scientific Charge-Coupled Devices", Opt. Eng. Vol 26, No. 8, 692-714 (1987).

3. R. D. McGrath, "Radiation Effects in a Virtual Phase CCD Imager", IEEE Trans. Nucl. Sci. NS-28, 4028-4032 (1980).

4. J.R. Srour, R.A. Hartman, S. Othmer, "Transient and Permanent Effects of Neutron Bombardment On A Commercially Available N-Buried Channel CCD", IEEE Trans. Nucl. Sc. NS-27, 1402-1410 (1980).

5. J. Janesick, T. Elliot, F. Pool, "Radiation Damage In Scientific Charge-Coupled Devices", IEEE Trans. Nucl. Sci. 36, 572-578 (1989).

6. T. Roy, S.J. Watts, D. Wright, "Radiation Damage Effects on Imaging Charge Coupled Devices", Nucl. Instr. and Meth. A275 545-557 (1989).

7. J.M. Killiany, "Radiation Effects on Silicon Charge-Coupled Devices", IEEE Trans. on Comp., Hybrids and Manuf. Tech. CHMT-1 353-364 (1978).

8. J.R. Srour, S.C. Chen, S. Othmer, R.A. Hartmann, "Neutron Damage Mechanisms in Charge Transfer Devices", IEEE Trans. Nucl. Sc. 25, 1251-1260 (1978).

9. G.R. Hopkinson, "Proton Damage Effects in an EEV CCD Imager", IEEE Trans. Nucl. Sc. Vol. 36, No. 6, 1865-1871 (1989).

10. M.W. Bautz, G.E. Berman, J.P. Doty, G.R. Ricker, "Charge-Coupled-Device X-Ray Detector Performance Model", Optical Engineering 26, 757-765 (1987).

11. D.H. Lumb, G.R. Hopkinson, A.A. Wells, "Performance of CCDs for X-Ray Imaging and Spectroscopy", Nucl. Instr. and Meth. 221, 150-158 (1984).

12. G. Fiorucci, J.-P. Bourquin, D. Bovet, E. Bovet, J.-P. Egger, C. Heche, C. Nussbaum, D. Schenker, D. Varidel, J.-M. Vuilleumier, "CCDs as Low-Energy X-Ray Detectors I. General Description", Nucl. Instr. and Meth. A292, 141-146 (1990).

13. D. Varidel, J.-P. Bourquin, D. Bovet, G. Fiorucci, D. Schenker, "CCDs as Low-Energy X-Ray Detectors II. Technical Aspects", Nucl. Instr. and Meth. A292, 147-155 (1990).

14. R. Clarke, B. Rodricks, R. Smither, "Virtual Phase CCD X-Ray Detectors", Rev. Sci. Instrum. 60, 2280-2283 (1989).

15. B. Rodricks, R. Clarke, R. Smither, A. Fontaine, "A Virtual Phase CCD Detector For Synchrotron Radiation Applications", Rev. Sci. Instr. Vol 60, No. 8, 2586-2591 (1989).

16. R. Clarke, "Use of CCD Detectors for Spectroscopy and Scattering Experiments", Nucl. Instr. and Meth. A291, 117-122 (1990).

17. R. Bailey, C.J.S. Damerell, R.L. English, A.R. Gillman, A.L. Lintern, S.J. Watts, F.J. Wickens, "First Measurement of Efficiency and Precision of CCD Detectors for high Energy Physics", Nucl. Instr. and Meth. 213, 201-215 (1983).

18. C.J.S. Damerell, F.J. Farley, A.R. Gillman, F.J. Wickens, "Charge-Coupled Devices for Particle Detection with High Spatial Resolution", Rutherford and Appleton Laboratories Report RL-80-082, October (1980).

19. C.W. Akerlof, J.W. Chapman, I. Gialas, W.A. Koska, D.F. Nitz, B.G. Rodricks, R.S. Tschirhart, "The Performance of "Virtual Phase" CCDs as Detectors of Minimum-Ionizing Particles", Nucl. Instr. and Meth. A260, 80-100 (1987).

20. M. Algranati, A. Faibis, R. Kaim, Z. Vager, "Use of Charge Transfer Device For Particle Detection", Nucl. Instr. and Meth. 164, 615-616, (1979).

21. S-B Ko, "Observation Of Alpha Particle Effects In The Charge-Coupled Image Sensor", IEEE Trans. Nucl. Sci. NS-27, 1500-1505 (1980).

22. L.K. Turner, D.S. Mantus, Y-C Ling, M.T. Bernius, G.H. Morrison, "Development and Characterization of Charge-Coupled Device Detection System For Ion Microscopy", Rev. Sci. Instrum. 60, 886-894 (1989).

23. P. Seige, G. Ress, "Application of Texas Instruments TC-104 Linear Charge-coupled-Device Arrays In Spaceborne Camera Systems", Optical Eng. 26, 1029-1034 (1987).

24. E.F. Rybaczewski, "Virtual-Phase Structure Simplifies Clocking For CCD Image Sensor", Electronics 55, No. 8, 141-144 (1982).

25. J. Hynecek, "Virtual Phase Technology: A New Approach to Fabrication of Large-Area CCDs", IEEE Trans. Elec. Dev. ED-28, 483-489 (1981).

26. J.R. Janesick, J. Hynecek, M.M. Blouke, "A Virtual Phase Imager For Galileo", in "Solid State Imagers for Astronomy", J.C. Geary and D.W. Latham, eds., Proc. SPIE 290, 165-173 (1981).

27. H.U. Keller, et al., "The Giotto Multicolor Camera", European Space Agency Report SP-1077, 149-172 (1986).

28. M. Courtois, G. Weill, "The SPOT Satellite System", in "Monitoring the Earth's Ocean, Land and Atmosphere from Space-Sensors, Systems and Applications", A. Schnapf, ed., 493-523, Am. Inst. Aeronaut. Astronaut., New York (1985).

29. J.H. Hubbel, "Photon Cross Sections, Attenuation Coefficients, and Energy Absorption Coefficients From 10 keV to 100 GeV", U.S. Department of Commerce, National Bureau of Standards publication NSRDS-NBS 29, Washington, D.C., August 1969.

UNCLASSIFIED

SECURITY CLASSIFICATION OF FORM

(highest classification of Title, Abstract, Keywords)

DOCUMENT CONTROL DATA

(Security classification of title, body of abstract and indexing annotation must be entered when the overall document is classified)

1. ORIGINATOR (the name and address of the organization preparing the document. Organizations for whom the document was prepared, e.g. Establishment sponsoring a contractor's report, or tasking agency, are entered in section 8.)

Defence Research Establishment Ottawa
Ottawa, Ontario
K1A 0Z4

2. SECURITY CLASSIFICATION (overall security classification of the document including special warning terms if applicable)

UNCLASSIFIED

3. TITLE (the complete document title as indicated on the title page. Its classification should be indicated by the appropriate abbreviation (S,C or U) in parentheses after the title.)

INVESTIGATION OF ALPHA PARTICLE INDUCED SINGLE-EVENT UPSETS IN CHARGE-COUPLED DEVICES (U)

4. AUTHORS (Last name, first name, middle initial)

PEPPER, GARY, T., AND FECHETE, ANDREW

5. DATE OF PUBLICATION (month and year of publication of document)

DECEMBER 1991

6a. NO. OF PAGES (total containing information. Include Annexes, Appendices, etc.)

47

6b. NO. OF REFS (total cited in document)

29

7. DESCRIPTIVE NOTES (the category of the document, e.g. technical report, technical note or memorandum. If appropriate, enter the type of report, e.g. interim, progress, summary, annual or final. Give the inclusive dates when a specific reporting period is covered.

DREO Report

8. SPONSORING ACTIVITY (the name of the department project office or laboratory sponsoring the research and development. Include the address.

NUCLEAR EFFECTS SECTION

9a. PROJECT OR GRANT NO. (if appropriate, the applicable research and development project or grant number under which the document was written. Please specify whether project or grant)

PROJECT 041LS

9b. CONTRACT NO. (if appropriate, the applicable number under which the document was written)

10a. ORIGINATOR'S DOCUMENT NUMBER (the official document number by which the document is identified by the originating activity. This number must be unique to this document.)

DREO REPORT 1114

10b. OTHER DOCUMENT NOS. (Any other numbers which may be assigned this document either by the originator or by the sponsor)

11. DOCUMENT AVAILABILITY (any limitations on further dissemination of the document, other than those imposed by security classification)

(X) Unlimited distribution
( ) Distribution limited to defence departments and defence contractors; further distribution only as approved
( ) Distribution limited to defence departments and Canadian defence contractors; further distribution only as approved
( ) Distribution limited to government departments and agencies; further distribution only as approved
( ) Distribution limited to defence departments; further distribution only as approved
( ) Other (please specify):

12. DOCUMENT ANNOUNCEMENT (any limitation to the bibliographic announcement of this document. This will normally correspond to the Document Availability (11). however, where further distribution (beyond the audience specified in 11) is possible, a wider announcement audience may be selected.)

Unlimited Announcement

UNCLASSIFIED

SECURITY CLASSIFICATION OF FORM

UNCLASSIFIED

SECURITY CLASSIFICATION OF FORM

13. **ABSTRACT** (a brief and factual summary of the document. It may also appear elsewhere in the body of the document itself. It is highly desirable that the abstract of classified documents be unclassified. Each paragraph of the abstract shall begin with an indication of the security classification of the information in the paragraph (unless the document itself is unclassified) represented as (S), (C), or (U). It is not necessary to include here abstracts in both official languages unless the text is bilingual).

The mechanisms for generation of single-event upsets (SEUs) in a linear charge-coupled device (CCD) were studied through irradiation with monoenergetic 5.48 MeV alpha particles from a very low flux ^{241}Am source. Spatial correlation ("cluster" analysis) of soft errors due to single alpha particle hits was demonstrated to be a necessary prerequisite for quantitative analysis of different SEU error-generating phenomena. The Texas Instruments TC-103 virtual phase CCD used in this study is shown to be sensitive to alpha particles not only in the vicinity of photosites as expected, but also in the transport CCDS. This latter effect may have adverse consequences for applications employing CCDs as position-sensitive ionizing radiation detectors. The techniques developed in this work for the analysis of one dimensional arrays is readily extensible to two dimensional CCD arrays.

14. **KEYWORDS, DESCRIPTORS or IDENTIFIERS** (technically meaningful terms or short phrases that characterize a document and could be helpful in cataloguing the document. They should be selected so that no security classification is required. Identifiers, such as equipment model designation, trade name, military project code name, geographic location may also be included. If possible keywords should be selected from a published thesaurus. e.g. Thesaurus of Engineering and Scientific Terms (TEST) and that thesaurus-identified. If it is not possible to select indexing terms which are Unclassified, the classification of each should be indicated as with the title.)

SINGLE-EVENT UPSET
CHARGE-COUPLED DEVICE
POSITION-SENSITIVE DETECTOR
RADIATION EFFECTS ON ELECTRONICS
CCD
LINEAR CCD